Journal of Nuclear Materials 377 (2008) 243–252

Contents lists available at ScienceDirect

Journal of Nuclear Materials

journal homepage: www.elsevier.com/locate/jnucmat

The electrical impedance response of steel surface oxide layers in molten lead–bismuth eutectic

James F. Stubbins *, Alan Michael Bolind, Xiang Chen

Department of Nuclear, Plasma, and Radiological Engineering, University of Illinois at Urbana-Champaign, Nuclear Engineering Laboratory, 103 South Goodwin Avenue, Urbana, IL 61801, USA

A B S T R A C T

Stainless steel 316L samples were preoxidized and then immersed in molten lead–bismuth eutectic (LBE) alloy at 200 °C. The changes in their electrical impedance responses were observed over time. Negligible impedance magnitudes were observed at first, followed by a rapid increase to thousands of ohm-cm^2. The impedance response is sensitive to changes in the immersed sample area. Micro-indentations on samples caused their impedance magnitudes to decrease initially, but the magnitudes recovered within a few days. SEM analysis showed that the indentations were still present and visible even after the recovery of impedance response, demonstrating that the physical features of the oxide layers which govern the electrical response must be smaller than the micrometer length scale.

1. Background

Molten lead–bismuth eutectic alloy (LBE) has been used successfully as a target in a particle accelerator, for the production of spallation neutrons [1]. A main advantage of using liquid LBE is that it can be pumped out of the target area to a heat exchanger, cooled there, and then pumped back into the target area. In this way, the LBE doubles both as the source for spallation neutrons and as its own coolant for the heat generated by the particle beam and the spallation reactions. One drawback of using LBE in this application is that it can significantly corrode the surfaces of the steel vessel and pipe containing the LBE. A popular method to mitigate this corrosion is to form protective oxide layers on the steel surfaces. However, these oxide layers must be actively maintained, and it is impossible while the accelerator system is operating to inspect visually the steel surfaces to verify that the oxide is present and protecting the steel. The use of the technique of impedance spectroscopy to measure the electrical impedance response of any oxide layers that may be present may be a solution to this monitoring problem. If negligible impedance is measured, then oxide may not be present; but if significant impedance is measured, then the oxide is almost sure to be present and protecting the steel surfaces from corrosion. Some work to characterize the impedance responses of such protective oxide layers has already been conducted, but more work was needed – and still needs – to be done in this area.

2. Motivation for this present investigation

In 2004, Lillard, et al., published an article on the relationships between the electrical impedance of oxide scales on martensitic and austenitic steels and their corrosion rates in liquid lead–bismuth eutectic (LBE) [2]. The main thrust of their work was to measure the electrical impedances of oxidized steels immersed in LBE and to use the corresponding conductivity values along with Wagner's oxidation theory to calculate corrosion rates for these steels [3,4]. These calculated rates were then compared with the sample thicknesses as observed by cross-sectioning the samples and examining them using scanning electron microscopy (SEM). In addition to varying the material (i.e., the elemental composition of the steel alloy), these authors also varied (1) the duration of preoxidation (in air at 800 °C) of the steels and (2) the temperature of the LBE. It was found that a threshold existed for preoxidation time, below which the oxide resistance was negligibly small, and that oxide resistance decreased with increasing LBE temperature.

Observed but not investigated in detail in the Lillard article was the dependence of the impedance responses of the samples upon the duration of immersion in LBE. It appeared that the impedance of any given sample began small, then increased rapidly, and finally increased much more slowly and steadily. Also, the impedances were measured for less than 200 h of LBE immersion. This time-dependence, therefore, became the initial focus of the present investigation. After obtaining such initial data and information, the focus shifted to conducting various experiments to determine the sensitivity of the results to variations in setup and to mechanical damage to the oxide layers. Such experiments would also explore mechanical – rather than chemical or electrical – explanations for the time-dependent behavior observed.

* Corresponding author.
E-mail address: jstubbin@uiuc.edu (J.F. Stubbins).

0022-3115/$ - see front matter © 2008 Published by Elsevier B.V.
doi:10.1016/j.jnucmat.2008.02.091

In addition to comparisons with the results Lillard article, the present results have also been compared with the results from impedance measurements made on oxide films formed from high-temperature oxidation of stainless steel 304 in gaseous environments [5,6]. Despite the slight difference in steel composition, some of these gaseous corrosion results can be compared almost directly with the preoxidation results of the present investigation. The post-immersion results, on the other hand, should be expected to be somewhat different, due to the corrosive and oxidative effects of the LBE over time. Nevertheless, the similarities between the results provide increased confidence in the results of the present investigation.

3. Experimental setup

A setup similar to that used by Lillard, et al., was used in the present investigation. An amount of LBE between two and three liters was kept at 200 °C and was open to air. (The LBE was stagnant, not stirred, however.) The LBE was contained in a ceramic liner in a stainless steel retort, in order to have a floating ground system for the purpose of eliminating electrical ground loops that would affect impedance measurements.

The samples were made of stainless steel 316L (6.5 cm × 0.635 cm × 0.76 mm = 2.5 in. × 0.25 in. × 0.03 in.), were sanded to a finish of 600 grit, and were cleaned in acetone, ethanol, and deionized water. They were then preoxidized for either 48 or 60 h approximately in a tube furnace at 800 °C under flowing air that was saturated with water vapor at room-temperature before entering the furnace. After preoxidation, one end of each sample was sanded to bare metal, where a wire was spot-welded onto it. Each sample was hung from its wire and dipped approximately half of its length into the molten LBE. Careful attention was paid to preventing electrical short-circuits. For this reason, each wire was threaded through an insulating ceramic tube.

The equipment package used to measure the impedance responses of the samples was manufactured by Princeton Applied Research and Signal Recovery (both currently owned by Ametek) and consisted of a Model 273A/92 potentiostat/galvanostat with a Model 5210 dual-phase, analog, lock-in amplifier. This system is capable of measuring impedances over the frequency range from 10 μHz to 100 kHz. The potentiostat is also able to provide signal currents up to 1.0 A approximately. Three terminals were used for measurements: the working electrode (i.e., the sample), the counter electrode (a bare metal rod dipped into the LBE), and a reference electrode (another such rod). The equipment were controlled and the data were collected by a PC running PowerSine® software, developed by Princeton Applied Research. Data were analyzed using ZView® software, developed by Scribner Associates, Inc.

4. Initial characterization of the time-dependence of the impedance response of oxide-covered steel samples

4.1. Impedance measurements

The impedance responses of undamaged samples (i.e., samples which were not intentionally mechanically damaged) were obtained by periodically scanning each sample over a range of signal frequencies (100 kHz to 100 mHz), using the equipment described previously. (Further information on the technique of impedance spectroscopy can be found in Refs. [7–10].) Figs. 1 and 2 show the impedance response of a typical sample. (For the purposes of this article, this sample will be referred to herein as Sample A. It was preoxidized for 48 h.) Part (a) of Fig. 1 is a complex plane plot, also commonly called a Nyquist plot; it plots the imaginary impedance (reactance) against the real impedance (resistance). (Note that what is plotted here is actually the negative of the imaginary impedance, since usually only capacitance, not inductance, is important in these types of experiments.) Parts (b) and (c) are the Bode plots, plotting firstly the magnitude of the impedance against signal frequency and secondly the phase angle of the impedance against signal frequency. The impedance responses at several different times are shown in all three parts of Fig. 1 so as to give the reader an impression of how the duration of the immersion of a sample affects its impedance response. Lastly, Fig. 2 takes the impedance at a single frequency – in this case, 1 Hz – and plots

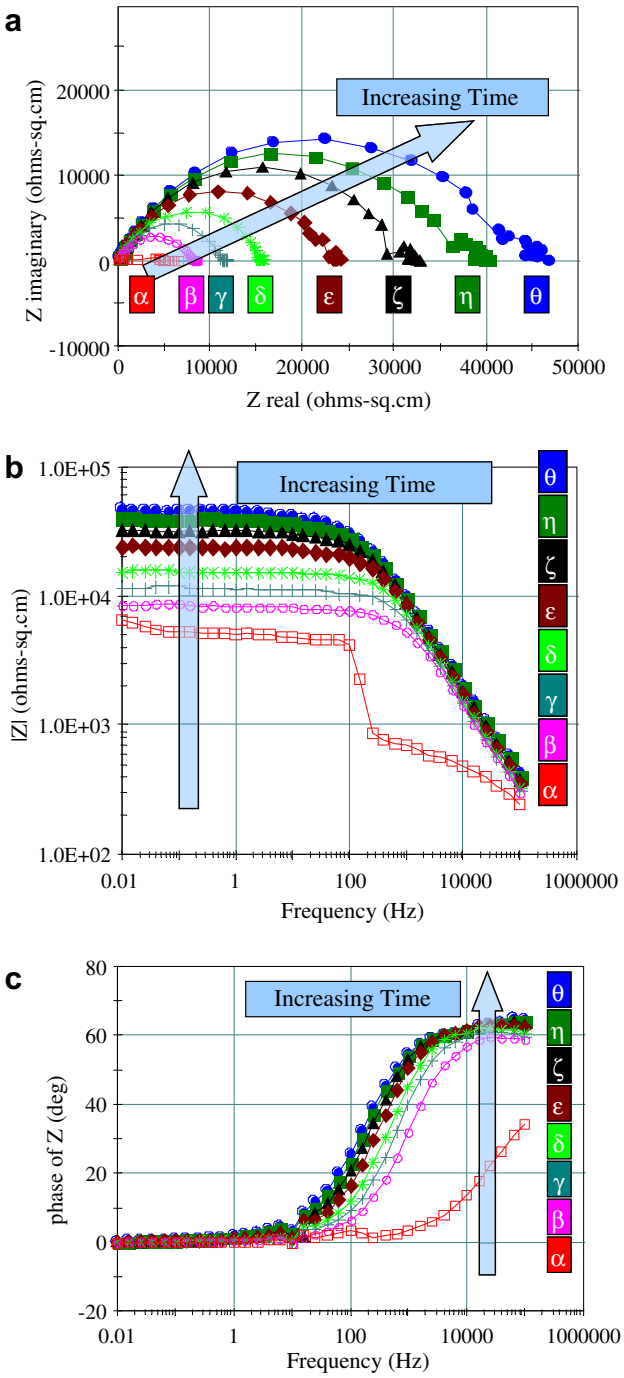

Fig. 1. Plots of the impedance response of a typical sample (Sample A). Curves represent impedance spectra at various durations of sample immersion and are denoted by Greek letters. (a) Nyquist plot, (b) Bode magnitude plot, (c) Bode phase plot.

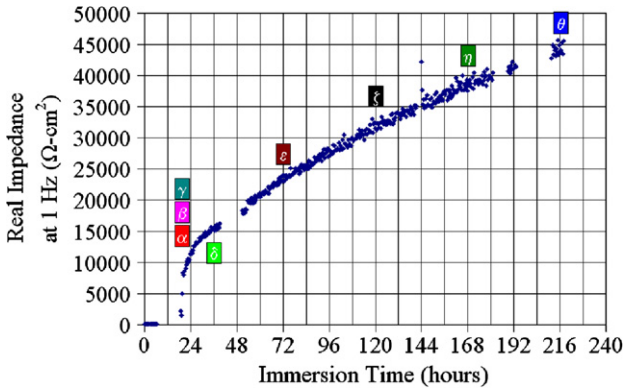

Impedance Scan	Time of Scan	Δ Between Scans
α	at 19.6 hours	
β	at 20.0 hours	24.6 minutes
γ	at 24.1 hours	4.1 hours
δ	at 35.9 hours	11.8 hours
ε	at 72.1 hours	36.1 hours
ζ	at 120.2 hours	48.1 hours
η	at 168.3 hours	48.1 hours
θ	at 217.7 hours	49.5 hours

Fig. 2. The effect of the duration of immersion on the impedance of a typical sample (Sample A). The values shown are the real impedance values taken at a signal frequency of 1 Hz. This plot corresponds to those in Fig. 1.

it as a function of time to give an even better picture of the effect of sample immersion time. To help connect the data between Figs. 1 and 2, Greek letters are used to indicate plots or points taken from the same impedance scans at the same times. Notice that in all these plots, the impedance values are area-normalized. The exact immersed areas of the samples were not measured, but an estimate based on immersion to half of the sample length was used (i.e., 4.7 cm^2).

The results at shorter immersion times and low-impedance magnitudes – represented by the data presented on Sample A – resembled, on the whole, the results obtained by Lillard, et al. The values for the area-normalized real impedance seem to be larger overall, in comparison with the data plotted in Fig. 8 in Lillard's paper. However, the area used to normalize the data of this investigation was estimated, as mentioned before. Also a significant variability of impedance magnitude was observed from sample to sample, even after accounting for different initial delay periods for significant impedance to develop. The responses also resembled those simulated from a Randles equivalent-circuit model of the physical system, especially at low impedance magnitudes. A simple Randles model is the circuit presented in Fig. 3; Lillard, et al., also used this equivalent circuit (Fig. 3 in their paper). A slightly modified Randles circuit uses a constant phase element (CPE) instead of a capacitor. The equations for the impedance produced by a capacitor and by a CPE are as follows:

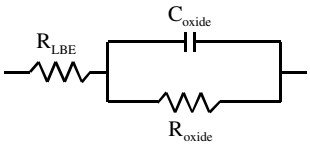

Fig. 3. Randles equivalent electrical circuit. C_{oxide} could be either a capacitor or a constant phase element.

$$Z_{capacitor} = \frac{1}{C(i\omega)} \text{ and } Z_{CPE} = \frac{1}{T(i\omega)^p}.$$

The reader should note that a capacitor is equivalent to a CPE with the exponent, p, equal to one, that C is the capacitance for the capacitor, and that T is the analogue of capacitance for the CPE. As the labels in Fig. 3 indicate, the parallel resistor–capacitor sub-circuit is interpreted to represent the capacitance and resistance of the oxide layers on the sample. The series resistor represents the resistance of the LBE from the sample to the counter electrode; this resistance is expected to be very low and almost negligible. Fig. 4 shows fits to the curve θ of Sample A from Figs. 1 and 2, as calculated by the ZView® software and using these two equivalent circuits. The Randles circuit with the capacitor does not fit curve θ well, but the Randles circuit with the CPE fits fairly well. Calculated values

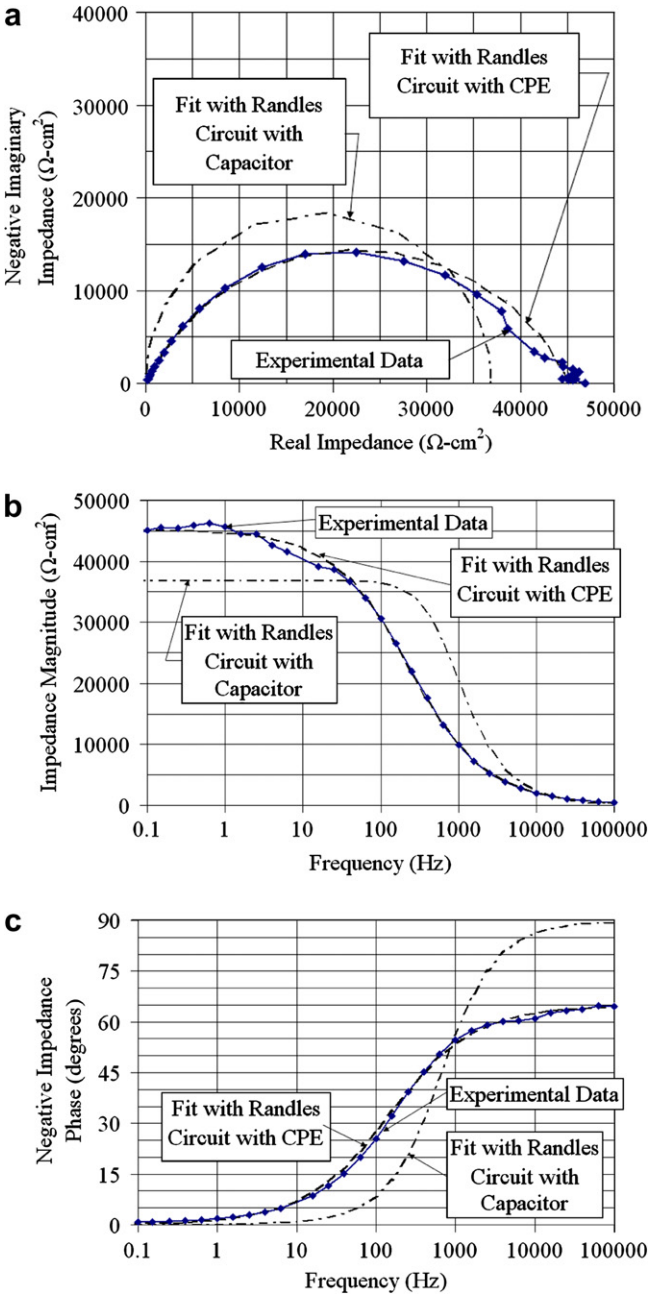

Fig. 4. Plots and equivalent-circuit fits for Sample A (curve θ of Figs. 1 and 2; after 218 h in LBE). (a) Nyquist plot, (b) Bode magnitude plot, (c) Bode phase plot.

Table 1
Fitted values of the equivalent circuit components shown in Fig. 3, for the fitted curves in Figs. 4 and 6

Sample	Figure	Fit	R_{oxide} (Ω-cm^2)	(C or T)$_{oxide}$ (nF/cm^2)	CPE exponent
A	4	With capacitor	36 800	6.5	1
A	4	With CPE	45 200	160.7	0.722
B	6	With capacitor	626 100	3.9	1
B	6	With CPE	720 800	19.7	0.840

for the components of the Randles equivalent circuits are given in Table 1.

As mentioned before, Fig. 2 shows the change in real impedance (i.e., resistance) as a function of time, at a measurement frequency of 1 Hz. As can be seen from the Bode phase plots (part (c), Fig. 1), the impedance at low frequencies is almost pure resistance; and the Bode magnitude plots (part (b), Fig. 1) show that the magnitude of this resistance is practically constant with frequency in this low-frequency region. In other words, the DC resistance and the low-frequency impedance are practically the same (especially at overall low impedance magnitudes). Further, since the greatest impedance magnitudes are measured at low frequencies (part (b), Fig. 1), a plot of the low-frequency impedance as a function of time shows how the overall magnitude of the impedance response changes with time. This rationale is the significance of Fig. 2.

From Fig. 2, then, it can be seen that a sample typically has very low impedance (i.e., the magnitude of the impedance is small) when the sample is first immersed in LBE. This condition occurs despite the fact that the sample is preoxidized and is, therefore, completely covered with an adherent oxide layer. What is not obvious from Fig. 2 and is not shown in Fig. 1 is that the impedance response at this low magnitude has practically no shape. In other words, the data points at all frequencies fall almost on top of each other on the Nyquist plot. The imaginary impedance is almost zero at all frequencies, so there is no semicircle, and the data cannot, therefore, be fitted to a Randles equivalent circuit. This response is identical with the response of a bare metal wire or sample – i.e., steel with no oxide on it – immersed in LBE and is seen regardless of the immersed area. The absolute resistance – i.e., the measured resistance, not normalized to the immersed area – in all these cases is less than 15 ohms, and is usually about 1 ohm. For practical intents and purposes, therefore, the impedance of newly immersed samples is negligible.

It is only after a sample has been immersed in LBE for several hours or even a few days that the magnitude of its impedance increases, appreciable imaginary impedance develops, and the Nyquist plot begins to take shape as a semicircle. This initial delay period for Sample A is shown in Fig. 2, and the transition to a significant impedance response can be seen in Figs. 1 and 2 as curves α and β. In the hours before curve α, some small increase in impedance began to be seen. Curve α appears as a line on the real axis of the Nyquist plot because the rapid increase in impedance magnitude and the development of significant imaginary impedance occurred while the impedance spectrum was being scanned (from high frequency to low frequency). The main jump occurred while the impedance at 158.5 Hz was being measured, as can be seen clearly in the Bode magnitude plot (part (b), Fig. 1). The time period from the previous frequency (251.2 Hz) to the following frequency (100.0 Hz) was 27 s; the entire jump occurred within this time period. The next spectrum to be scanned (curve β) began 9 min, 38 s, after the end of the previous spectrum, and by this time, the impedance response had developed fully into the standard semicircle of a Randles equivalent circuit. The exact frequencies and times mentioned here are unimportant; the important observation is that the development of a significant impedance response in a sample can occur rapidly, with large jumps occurring within a period of seconds. These experimental observations provide further information and clarity of the phenomenon reported by Lillard, et al., in Fig. 7 of their paper, namely, that there is a threshold preoxidation time for a sample, below which it has negligible impedance. While this interpretation may be true, it is also clear from the present investigation that a sample may not develop significant impedance until after an initial delay period. In other words, some of the preoxidized samples which Lillard, et al., reported as having no impedance might actually have developed a significant impedance response if they had been left immersed in LBE for a longer period of time. In the experience of the present investigators, a waiting period of at least three days, perhaps even longer, is necessary to determine whether or not a sample will develop significant impedance.

Another feature of the time-dependence of the impedance response is that the rate of increase of the impedance magnitude is not constant but can vary. In Fig. 2, a fit to the data after the initial jump just described previously shows that the impedance of Sample A has a parabolic dependence upon time. Some other samples, however, do not show such a parabolic dependence; the impedance may increase linearly or with some other polynomial dependence. Even for a particular sample, the rate can spontaneously change for no apparent reason. At this point, therefore, it cannot be predicted what the time-dependence of impedance of a given sample will be, after the initial jump in impedance. Further work needs to be done to characterize these rates, especially at longer immersion times.

At longer immersion times, the impedance responses shift somewhat. Fig. 5 shows the impedance response of another sample over a much longer duration of immersion. (This sample is denoted herein as Sample B. It was preoxidized for 61 h.) At long immersion times and high impedance magnitudes, Sample B's Nyquist plots are elongated, and its Bode magnitude plots slope gently downward at low frequency and transition without a shoulder to the angled mid-portion of the standard backwards-S-shaped curve for a Randles circuit.

Fig. 6 also shows the impedance spectrum of Sample B after it had been immersed in LBE for 30 days, as compared to the 218 h of immersion for curve θ of Sample A. Neither the Randles circuit with a capacitor nor the Randles circuit with the more general CPE can fit this spectrum well, failing especially to fit the elongation on the Nyquist plot. (See Table 1 for calculated values of the components of the Randles equivalent circuits.) Therefore, a more complex physical model of the oxide – and a corresponding new equivalent circuit – must be developed to account for the impedance responses of high-impedance oxides (i.e., oxides which have been immersed for long time periods and have overall larger impedance magnitudes at all frequencies), including the transition with time from low-impedance spectra to high-impedance spectra.

4.2. Microscopic examination of oxide surfaces

The surfaces of the oxides on several samples were examined using secondary electron microscopy (SEM). The samples were not examined prior to immersion in LBE, but only afterwards. This choice avoided the need to coat the samples with carbon or Pt/Au for SEM examination, which would be expected to influence the subsequent reactions when the samples were placed into the LBE. However, portions of each sample above the level of immersion (i.e., above the liquid line) were examined. These micrographs can be taken to represent the surface prior to immersion, as the relatively low temperature of the experiments (around 200 °C) would not allow the samples to undergo further oxidation in the air.

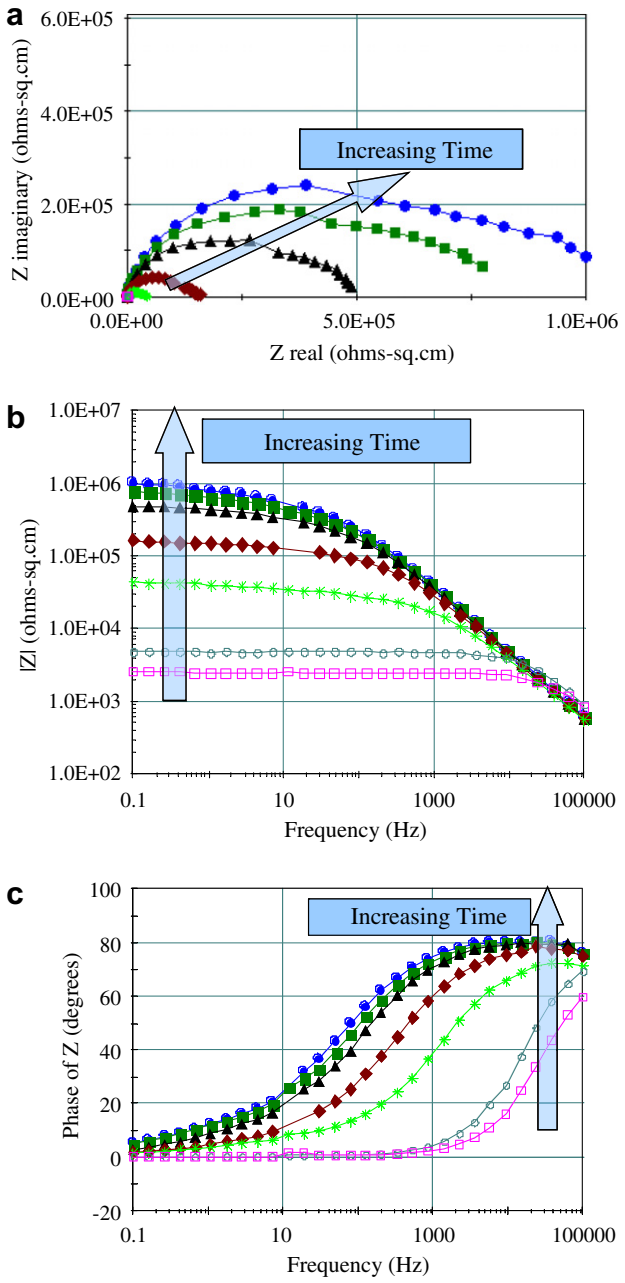

Fig. 5. Plots of the impedance response of a typical sample at larger impedance magnitudes (Sample B). The first curve is after 10.9 days of immersion; the second is 2.2 hours later; and the time between subsequent adjacent curves is approximately 4 days. (a) Nyquist plot, (b) Bode magnitude plot, (c) Bode phase plot.

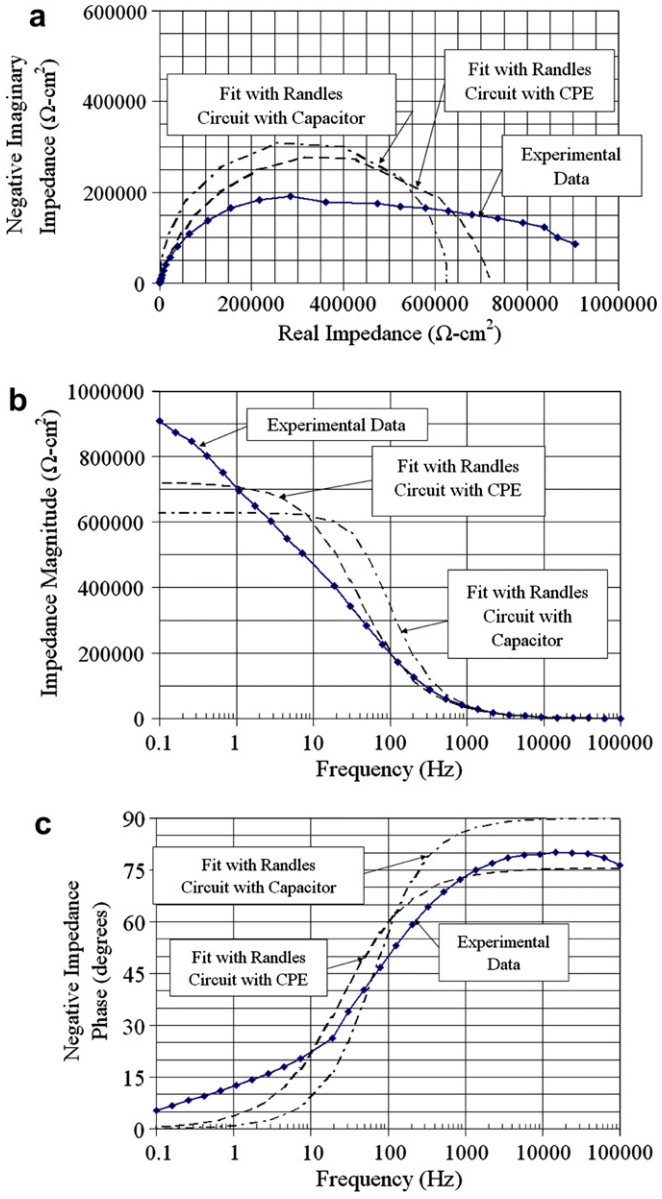

Fig. 6. Plots and equivalent-circuit fits for Sample B, after 30 days in LBE. (a) Nyquist plot, (b) Bode magnitude plot, (c) Bode phase plot.

When samples are pulled out of the liquid LBE, a thin film of LBE almost always adheres to the sample surface and solidifies as the sample cools. This film must be removed from the surface before the sample can be examined with SEM. For the present investigation, the cleaning method used by Kondo and Takahashi was modified and used to remove the LBE films [11]. Samples were removed from LBE and immersed in glycerin at a temperature between 160 °C and 190 °C, which is above the melting temperature of LBE (124 °C). Most of the LBE either formed droplets and rolled off the sample surface or was easy to rub off gently with a cotton swab. The samples were then removed from the glycerin and allowed to cool in air to room-temperature before being immersed successively in room-temperature baths of acetone and ethanol to remove residual glycerin. To provide confidence that the oxide surfaces were not altered by this cleaning process, one test sample (preoxidized but never immersed in LBE) was examined using an optical microscope (to 6204 times magnification) before and after cleaning. No visible change in the oxide surface characteristics was observed.

Fig. 7 presents two SEM micrographs of the oxide surface of a typical sample prior to immersion (i.e., above the liquid line). (This sample is denoted herein as Sample C. It was preoxidized for 66 h.) These micrographs are very similar to the micrographs of the surfaces of the high-temperature, gaseous-corrosion oxidation films formed on stainless steel 304, as reported by Pan, et al., and by Song and Xiao [5,6]. Fig. 8 is the corresponding micrographs of this sample after approximately 18 days of immersion in LBE. From these figures, it appears that the oxide crystals are more separated and well defined prior to immersion, whereas after immersion the crystals seemed to have clumped together, especially at their bases. Whether this clumping is due to the growing together of existing oxide crystals or to the formation and growth of new oxide

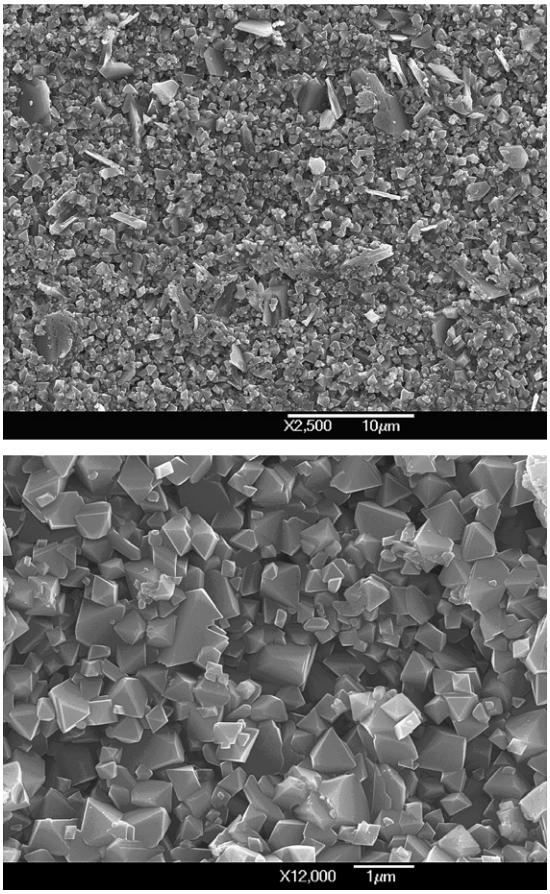

Fig. 7. SEM micrographs of the oxide surface of Sample C. The area shown here was above the liquid line (i.e., the oxide here was not immersed in LBE). The lower picture is a magnification of a portion of the upper picture.

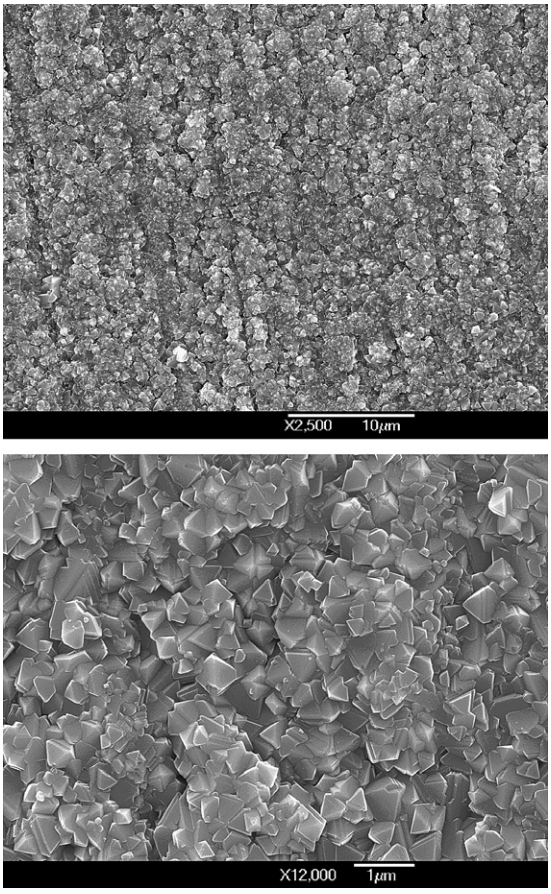

Fig. 8. SEM micrographs of the oxide surface of Sample C. The area shown here was below the liquid line (i.e., the oxide here was immersed in LBE). The lower picture is a magnification of a portion of the upper picture.

crystals in between the existing ones is not clear. The linear troughs seen in Fig. 8 were also seen in other samples in areas which had not been immersed in LBE. Since it appears as though these troughs were present both before and after immersion, they can be ruled out as having an effect on the time dependence of the impedance response. (The troughs may have originated in the 600-grit polishing of the steel surface prior to oxidation.) Lastly, Fig. 9 shows a portion of the sample surface that still contained residual LBE; the oxide crystals and the LBE crystals are easily distinguished from one another.

The above observation regarding the clumping or merging of oxide crystals during immersion in LBE has led to the hypothesis that this clumping is responsible for the increase in impedance magnitude of an immersed sample over time. Exactly how this clumping would increase the impedance is unclear, however. One idea is that, prior to clumping, the LBE flows in between the oxide crystals and closely approaches the steel substrate. In these cases, the electricity has a short distance of oxide – which is relatively non-conductive – through which it must travel to reach the relatively much more conductive LBE. After the oxide crystals clump together, the LBE does not reach as far in between the crystals, which forces the electricity to travel through much more of the oxide before it reaches the LBE. Therefore, the impedance would be expected to increase over time as the oxide crystals increasingly clump together. Pan, et al., used somewhat similar reasoning in their description of the defective and porous outer layer seen in their experiments, as well as in their description of how the impedance of their samples changed with time [5]. The problem with this idea is that SEM micrographs of the cross-sections of these samples do not show such clearly separated oxide crystals down to the substrate. Instead, a mostly uniform oxide of 2 μm thickness is seen. Perhaps, then, the clumping represents some other physical or chemical phenomenon which increases electrical impedance. Further experimentation and microanalysis is needed to investigate this problem.

4.3. Measured values of impedance versus values estimated from literature on bulk oxides

One important problem with the results presented so far regards the order of magnitude of the measured impedance responses. According to Samsonov's *The Oxide Handbook* [12], magnetite (Fe_3O_4), chromium oxide (Cr_2O_3), and nickel oxide (NiO) have specific electrical resistivity (ρ) values of 4.74×10^1 Ω-m (at 125 °C), 1.3×10^1 Ω-m (at 350 °C), and 6.70×10^1 Ω-m (at 590 °C), respectively. The oxide layers on the SS316L steel samples must be primarily a combination of one or more of these oxides. Therefore, a rough and conservatively large estimate of the electrical specific resistivity of the oxides on the steel samples can be taken as 10^2 Ω-m at 200 °C. Using also the average value of the oxide thickness – 2 μm – the area-normalized resistance ($R \cdot A$) can be estimated:

$$R \cdot A = \rho \cdot l = (10^2 \Omega \times \mathrm{m}) \bullet (2 \times 10^{-6}\ \mathrm{m}) = 2\Omega \times \mathrm{cm}^2.$$

This value of 2 Ω-cm^2 is several orders of magnitude smaller than the area-normalized resistance values measured by Lillard, et al.,

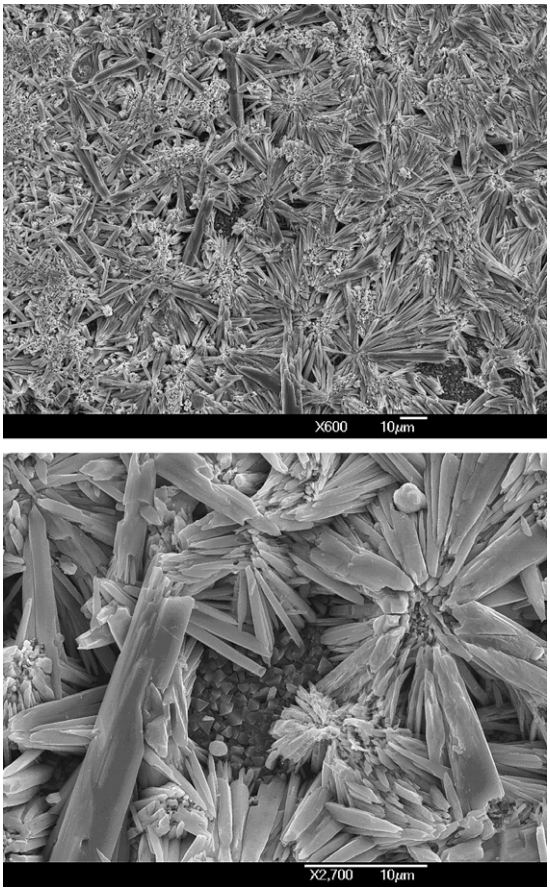

Fig. 9. SEM micrographs of a portion of the oxide surface of Sample C which still contained some residual LBE. The large, thin crystals are LBE; the small crystals are the underlying oxide. The lower picture is a magnification of a portion of the upper picture.

by Pan, et al., and by this present investigation (i.e., over the range of 10^2 to 10^6 Ω-cm^2). An initial and superficial explanation might be that actually lead oxide (PbO) – which has a specific resistivity of 10^7 Ω-m at 120 °C – is present in significant quantities on the sample surfaces and causes the large impedance magnitudes that have been observed. However, this situation cannot be the case, since the (steel) oxide crystals are clearly seen using optical microscopy and SEM both before and after immersion. Also, experiments were conducted (see the following description of the indentation experiments) in which samples were removed from the LBE, cleaned, and then put back into the LBE and immediately had several hundreds of ohm-cm^2 of impedance. Additionally, the experiments by Pan, et al., were gaseous corrosion experiments in which no LBE was used at all, yet they gave impedance results of similar magnitudes. Therefore, the measured impedance values cannot be caused by lead oxide; they must be caused by the (steel) oxide itself. Interestingly, the results given by Song and Xiao [6] seem to be closer to the order of magnitude estimated from the bulk oxides. These researchers used an 8 mm × 8 mm platinum foil for their electrical interface with the oxide, rather than an aqueous solution as used by Pan, et al. [5]. (Comparison with Song and Xiao's results is tentative because they did not area-normalize their data, but one can use the area of the platinum foil for an estimate). This fact indicates that experimental setup may be an important factor. Therefore, further investigation into the experiments behind the reported literature values and comparison of the various experimental techniques used to determine oxide electrical resistivity are necessary to resolve this apparent discrepancy.

5. Investigation of the sensitivity of oxide impedance response to mechanical changes

The initial experiments described above did not involve any changes to the setup once samples had been inserted into the molten LBE; the samples were left alone except for periodic scanning of the impedance spectra. It was important, however, to determine how sensitive the samples were to changes in the setup and to mechanical damage to the oxide layers. Such experiments might also provide additional information about the nature of the impedance responses.

5.1. The effects of removal and reinsertion of a sample

The first of these sensitivity experiments was simply to determine the effect of removing a sample, cleaning it, and putting it back into the LBE otherwise unchanged. In all cases, the impedance dropped precipitously upon re-immersion. In some cases, the low-frequency impedance (at 100 mHz) dropped below 50 ohms-cm^2, a negligible value and similar to the impedance of a fresh preoxidized sample when it is put into LBE for the first time. In other cases, the sample retained significant impedance after cleaning, on the order of several hundreds or even thousands of ohms-cm^2. In almost all cases, the impedance response eventually recovered and grew to large magnitudes and with the same characteristics, as before. In light of the next experiment to be described, it is important to mention that these effects were seen regardless of the depth to which the sample was re-immersed, whether more or less than the original depth.

5.2. The effects of a sudden increase in the immersed surface area

The next experiment involved establishing a steady, significant impedance response in a sample, then pushing the sample 5 mm further down into the LBE to immerse more of its surface area and seeing how the impedance response changed. Since more area was exposed with the new sample position, the impedance magnitude was expected to drop, because of the following rationale:

The impedance response of the surface area prior to the further immersion has been assumed to be described by a Randles equivalent circuit as described previously. Correspondingly, the additional, newly exposed surface area should also be able to be described by another Randles equivalent circuit, although with different values for the circuit components. Since the newly exposed area provides an additional conduction path for the electricity, this second Randles circuit should be considered to be in parallel electrically with the first Randles circuit, as shown in Fig. 10. From Kirchhoff's circuit laws, then, the total impedance of the sample at the new immersion depth is given as follows:

$$\frac{1}{Z_{\text{total}}} = \frac{1}{Z_1} + \frac{1}{Z_2} \quad \text{or} \quad Z_{\text{total}} = \frac{Z_1 Z_2}{Z_1 + Z_2} = \frac{Z_2}{1 + Z_2/Z_1}.$$

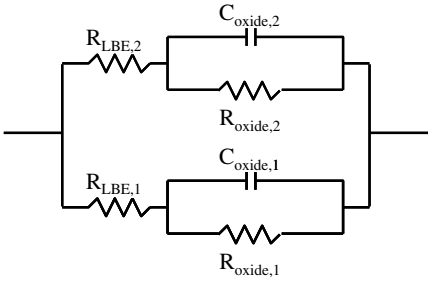

Fig. 10. Combination of two Randles circuits, representing two different areas of oxide which are in parallel electrically with each another.

Thus the new total impedance is less than the impedance of either the previously exposed surface area or the newly exposed surface area. In fact, the newly exposed surface area is expected to have less impedance than the previously exposed area, since prior experiments have shown that samples begin at low impedance and gain more impedance over time. The conclusion, then, is that the impedance of the entire sample at the new immersion depth should decrease significantly.

This experiment was conducted on Sample B, described previously, and the results are shown in Figs. 11 and 12. At point 1 in Fig. 11, the sample was immersed an additional 5 mm. The impedance of the sample dropped significantly, though not to a negligibly small value; this fact implies that the oxide of the newly exposed area had significant impedance. What is most surprising about the data in Figs. 11 and 12 is the practically instantaneous jump in impedance at point 2 in Fig. 11, to which Fig. 12 corresponds. The impedance returned to a level consistent with the general increasing trend that existed prior to the additional immersion. After this point, the sample appears to have behaved as though no additional immersion ever occurred. Moreover, the jump occurred during the middle of an impedance scan, as can be seen in Fig. 12. The time difference between the two data points bracketing the jump is only 9 s, a time period which is reminiscent of the jump described previously for curve α in Figs. 1 and 2. No explanation for this jump is presently known.

5.3. The effects of damage from micro-indentations

A third set of experiments involved intentionally damaging the oxide layer of a sample to see if its impedance would decrease. Samples were immersed in LBE until they achieved significant impedance magnitudes; then they were removed and cleaned. Next, they were each indented once using a microhardness indent-

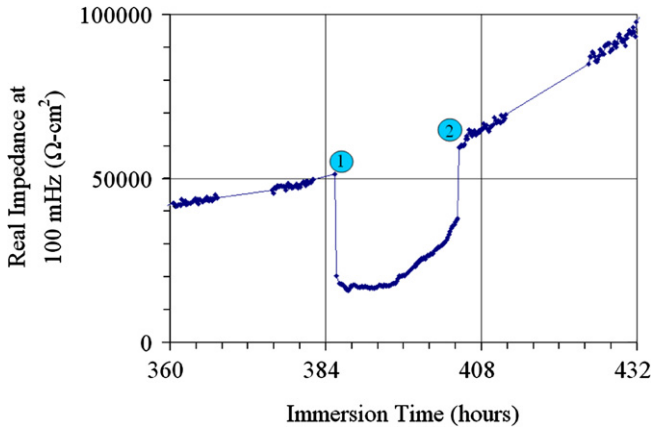

Fig. 11. The effect upon real impedance of immersing Sample B an additional 5 mm into LBE at the time indicated by ①. At time ②, the impedance recovered without human intervention.

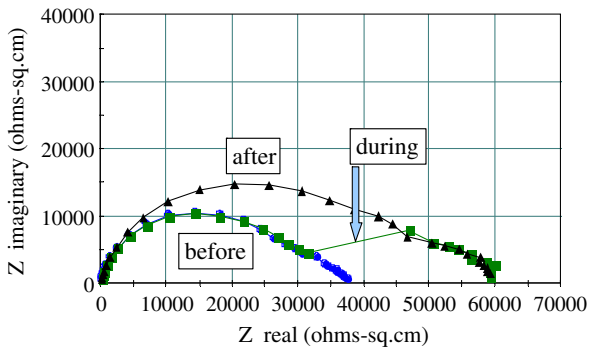

Fig. 12. Nyquist plots of the impedance spectra of Sample B immediately before, during, and after the regain of impedance at point 2 in Fig. 11.

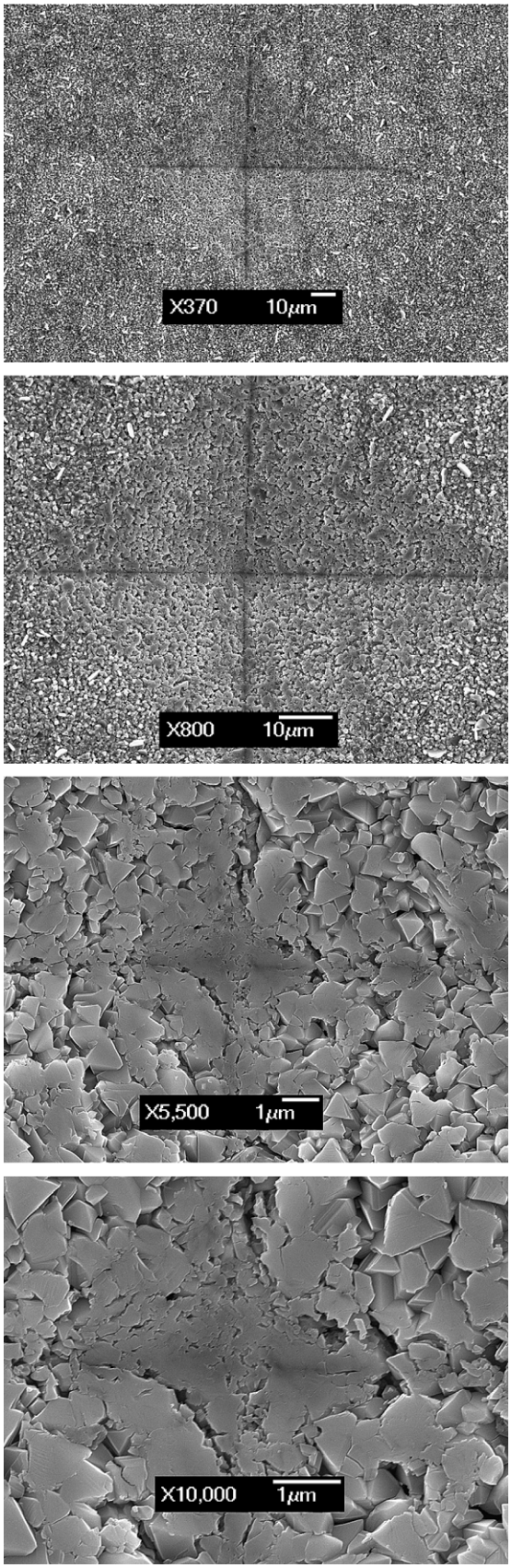

Fig. 13. SEM micrographs of an indentation in a sample, after the sample had been re-immersed for 4 days.

ing machine with a Vickers indenter. Indentations were done with 1000 g of force. Typical indentations measured approximately 80–90 μm along the diagonals, corresponding to Vickers hardness numbers between 200 and 300 and penetration depths of approximately 18 μm (calculated from the known standard angle between the faces of the Vickers indenter, namely, 136°). The samples were then re-immersed in LBE, and their impedance responses were measured.

Most indented samples behaved like non-indented samples which had simply been removed from LBE, cleaned, and re-immersed, as described above. They showed low impedance magnitudes initially upon re-immersion, but the impedance responses recovered to large magnitudes over time. Three indented samples were removed from the LBE, cleaned again, and examined with SEM. Typical micrographs from one of these samples are shown in Fig. 13.

Two main conclusions can be drawn from observation of these pictures. Firstly, the indentation is still clearly visible, even though the sample had been re-immersed for over four days and the impedance response had recovered. Therefore, the indentation as a whole did not cause the impedance loss observed immediately upon re-immersion of the sample; if it had, then it should be expected that the indentation must necessarily be 'filled in' or 'healed' in order for the impedance response to recover. Instead, oxide features with a length scale much smaller than that of the indentation (90 μm) must be primarily responsible for impedance loss and recovery. Secondly, the oxide must be slightly compressible and significantly pliable. The indenter penetrated approximately 18 μm into the sample surface, yet the oxide thickness was only about 2 μm. The higher magnification micrographs show that the oxide crystals – which can be clearly seen in their undamaged state in Figs. 7 and 8 – have been slightly compressed. The individual crystals are still visible, but it appears as though their tops have been flattened along the angled planes of the surface of the Vickers indenter. However, since the crystals are still visible, the steel substrate must have deformed much more than the oxide; i.e., the steel must be softer than the oxide, which is expected. Also, no cracks in the oxide are visible, even at the edges and corners of the indentation, where the stress caused by the indentation would have been greatest. Therefore, the oxide must be significantly pliable.

5.4. Conclusions from the sensitivity experiments

There are three main conclusions of these sensitivity experiments. First, the impedance response of a sample is sensitive to changes in immersed area, but only in the short term. Second, the oxide can withstand a small amount of damage and yet maintain its coverage of the steel substrate. It can also maintain its impedance magnitude or, at least, regain it after an initial period. Third, if physical features of the oxide (rather than chemical features) dominate the electrical impedance response of the oxide, these dominant features must be of a length scale smaller than micrometers.

6. Conclusions

The main intent of this investigation was to characterize the time-dependence of the impedance response of preoxidized stainless steel samples immersed in molten LBE. It has been found that preoxidized samples begin with negligible impedance and must undergo an initial waiting period before a significant impedance response develops. At the end of the waiting period, the impedance increases dramatically at first, and then increases more slowly and steadily, although the rate of increase can also subsequently and spontaneously change. It is also possible for the impedance to jump practically instantaneously – i.e., on the order of seconds.

At low overall impedance magnitudes, the impedance response follows the characteristics of the simple Randles equivalent circuit with a CPE. As the magnitude increases, the Nyquist plot of the impedance spectrum becomes elongated, and the Bode magnitude plot changes from being flat to having a slightly downward slope at low frequencies. Such impedance responses at high overall impedance magnitudes cannot be adequately modeled with a simple Randles circuit.

The oxide crystals on a sample can be clearly seen with SEM and are distinct from one another after preoxidation and before immersion in LBE. After immersion in LBE for several hours or days, the oxide crystals appear to have merged or clumped together at their bases. This clumping might be related to the increase of the impedance of the sample with time.

The magnitude of the impedance responses measured on preoxidzied stainless steel samples immersed in LBE is several orders of magnitude greater than that expected from a simple calculation based on reported literature values of the electrical resistivity of chromium, iron, and nickel oxides and an observed oxide thickness of 2 μm. This discrepancy may be due to differences in the experimental methods used to obtain the literature values.

The impedance response of a sample decreases dramatically if the sample is removed from the LBE, cleaned, and put back into the LBE, but oftentimes the sample will still have a non-negligible impedance response. The impedance response of a sample is also sensitive to changes in the immersed area, but only temporarily. Microscopic damage to a sample has only a temporary, if any, effect, and the oxide on a sample is slightly compressible and significantly pliable. Lastly, if physical features of the oxide (rather than chemical features) dominate the electrical impedance response of the oxide, the dominant features must be of a length scale smaller than micrometers.

The above observations and conclusions have important ramifications for any future use of impedance spectroscopy to measure the impedance of protective oxides on steel surfaces in contact with LBE in a liquid-LBE accelerator target. One possible setup might use a steel probe that is inserted into the vessel containing the LBE and serves as a representative surface for all the vessel surfaces in contact with the LBE [13]. The idea would be that if the probe surface has protective oxide on it then the vessel surfaces must also have protective oxide on them. That the probe surface has oxide on it can be verified at any time by scanning its impedance spectrum; if a significant impedance response is measured, then an oxide must be present. In this setup, then, the observations and conclusions of this present investigation lead to important operational practices and interpretation of the results of such an oxide-monitoring system. The probe may take several hours or days to begin to work after the empty vessel has been filled with LBE or after the probe has been inserted into a full vessel, because of the initial waiting period before a significant impedance response is developed. Also, to prevent a short-circuit to the steel vessel wall, the probe must be inside an electrically insulating ceramic sleeve or have some other such isolation with ceramic material. Because of the observation that the physical features which govern the increase in impedance response are smaller than the length scale of micrometers, the joint between the oxide-covered probe surface and the insulating ceramic material must be very good, lest a small area of steel substrate be uncovered or some other low-impedance conduction path be created at the joint. Also, the working surface of the probe should be completely immersed in the LBE at all times, to avoid any changes in impedance response due to changes in the immersed surface area. Lastly, the observation that microscopic damage on the order of a micrometer length scale does not permanently damage the oxide impedance is good

news: The probe probably will be able to withstand gentle handling and still work properly.

Acknowledgements

The authors would like to thank Ning Li and R. Scott Lillard from Los Alamos National Laboratory for their support and research guidance and contributions. Also, Eric P. Loewen (now at GE Energy) contributed valuable experimental expertise. This research was funded by a grant from Los Alamos National Laboratory (Contract No. 57384-001-02 8).

References

[1] F. Groeschel, C. Fazio, J. Knebel, C. Perret, A. Janett, G. Laffont, L. Cachon, T. Kirchner, A. Cadiou, A. Guertin, P. Agostini, J. Nucl. Mater. 335 (2004) 156.
[2] R.S. Lillard, C. Valot, R.J. Hanrahan, Corrosion (Houston) 60 (2004) 1134.
[3] P. Kofstad, High Temperature Corrosion, Elsevier Applied Science, London, 1988.
[4] C. Wagner, Z. Phys. Chem. 21 (1933) 25.
[5] J. Pan, C. Leygraf, R.F.A. Jargelius-Petterson, J. Lindén, Oxid. Met. 50 (1998) 431.
[6] S.-H. Song, P. Xiao, J. Mater. Sci. 38 (2003) 499.
[7] Basics of Electrochemical Impedance Spectroscopy, Princeton Applied Research. <www.princetonappliedresearch.com>, 2003 (accessed 4.26.03).
[8] A.T. Ltd., The Impedance Measurement Handbook: A Guide to Measurement Technology and Techniques, Agilent Technologies Co. Ltd., <http://cp.literature.agilent.com/litweb/pdf/5950-3000.pdf>, 2003 (accessed 11.16.05).
[9] E. Barsoukov, J.R. MacDonald, Impedance Spectroscopy: Theory, Experiment, and Applications, 2nd Ed., John Wiley & Sons, New York, 2005.
[10] M. Honda, H. Haruta, Agilent Technologies Impedance Measurement Handbook, 2nd Ed., Agilent Technologies Co. Ltd., 2000.
[11] M. Kondo, M. Takahashi, J. Nucl. Mater. 356 (2006) 203.
[12] G.V. Samsonov, The Oxide Handbook, 2nd Ed., IFI/Plenum, New York, 1982.
[13] R.S. Lillard, M. Paciotti, Conceptual Design of a Corrosion Probe for Use in Molten Lead–Bismuth Eutectic, LA-UR-03-0058, Los Alamos National Laboratory, Los Alamos, New Mexico, 2003.